A Cyclometalated Ir^{III} Complex Conjugated to a Coumarin Derivative Is a Potent Photodynamic Agent against Prostate Differentiated and Tumorigenic Cancer Stem Cells

Vojtech Novohradsky,[a] Lenka Markova,[a] Hana Kostrhunova,[a] Jana Kasparkova,[a] José Ruiz,[b] Vicente Marchán,[c] and Viktor Brabec*[a]

Abstract: A cyclometalated Ir^{III} complex conjugated to a far-red-emitting coumarin, Ir^{III}–COUPY (**3**), was recently shown as a very promising photosensitizer suitable for photodynamic therapy of cancer. Therefore, the primary goal of this work was to deepen knowledge on the mechanism of its photoactivated antitumor action so that this information could be used to propose a new class of compounds as drug candidates for curing very hardly treatable human tumors, such as androgen resistant prostatic tumors of metastatic origin. Conventional anticancer chemotherapies exhibit several disadvantages, such as limited efficiency to target cancer stem cells (CSCs), which are considered the main reason for chemotherapy resistance, relapse, and metastasis. Herein, we show, using DU145 tumor cells, taken as the model of hormone-refractory and aggressive prostate cancer cells resistant to conventional antineoplastic drugs, that the photoactivated conjugate **3** very efficiently eliminates both prostate bulk, differentiated and prostate, hardly treatable CSCs simultaneously and with a similar efficiency. Notably, the very low toxicity of Ir^{III}–COUPY conjugate in the prostate DU145 cells in the dark and its pronounced selectivity for tumor cells compared with noncancerous cells could result in low side effects and reduced damage of healthy cells during the photoactivated therapy by this agent. Moreover, the experiments performed with the 3D spheroids formed from DU145 CSCs showed that conjugate **3** can penetrate the inner layers of tumorspheres, which might markedly increase its therapeutic effect. Also interestingly, this conjugate induces apoptotic cell death in prostate cancer DU145 cells associated with calcium signaling flux in these cells and autophagy. To the best of our knowledge, this is the first study demonstrating that a photoactivatable metal-based compound is an efficient agent capable of killing even hardly treatable CSCs.

Introduction

Prostate cancer is the second most commonly occurring type of cancer in men worldwide. Among the different strategies available for treating prostate cancer,[1] chemotherapy is one of the most common options for men with advanced or aggressive prostate cancer.[2] Up to the present time, prostate cancer has been treated with different chemotherapeutic agents. However, conventional therapies exhibit several disadvantages, such as limited efficiency to target prostate cancer stem cells (CSCs), which are considered the main reason for chemotherapy resistance, relapse, and metastasis.[3] Hence, it is reasonable to expect that prostate cancer chemotherapy could be improved by introducing new chemotherapeutic agents that kill with substantial efficiency both differentiated prostate cancer cells and prostate CSCs.

CSCs, including prostate CSCs, possess low ROS levels,[4] and, consequently, drugs that can generate ROS are capable of inducing CSCs death.[5] We recently demonstrated[6] that conjugation between a cyclometalated Ir^{III} complex (**1**, Figure 1) to a far-red-emitting COUPY coumarin (**2**) generated a new anticancer agent, Ir^{III}–COUPY (**3**), with highly favorable properties for cancer phototherapy. Indeed, photocytotoxicity of this new photosensitizer agent clearly correlated with intracellular ROS generation after visible light irradiation. Additionally, Ir^{III}–COUPY exhibited high photocytotoxicity under biologically-compatible visible-light irradiation, both in normoxia and hypoxia, limiting the extent of unwanted side effects associated with high energetic wavelengths that significantly limit patient's life quality. Thus, photo-induced therapy with Ir^{III}–COUPY conjugates, such as photodynamic therapy (PDT), might provide a new approach for prostate cancer treatment due to its localized and controlled cytotoxic effect, as well as its low incidence of side effects and tumor resistance occurrence. Here we demonstrate that photoactivated Ir^{III}–COUPY conjugate (**3**) effectively eliminates both prostate bulk, differentiated and prostate CSCs simultaneously and with similar efficacy and describe some essential features of its mechanism of action.

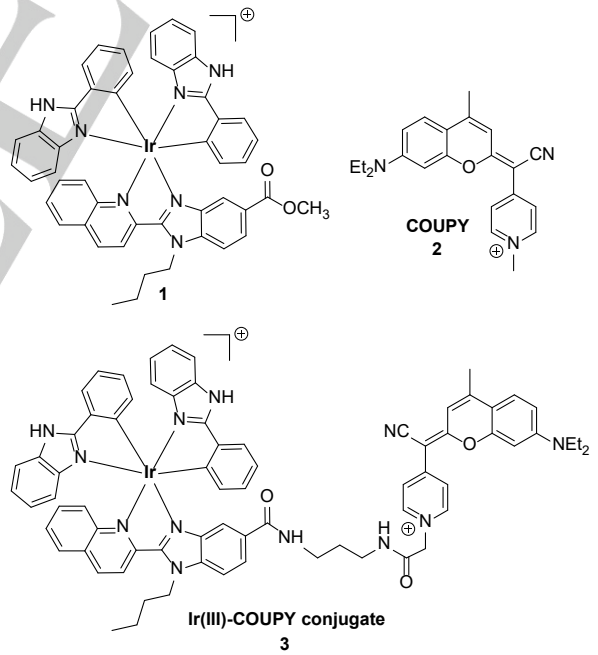

Figure 1. Structures of compounds investigated in this study.

[a] Dr. V. Novohradsky, Dr. L. Markova, Dr. H. Kostrhunova, Prof. Dr. J. Kasparkova, Prof. Dr. V. Brabec
Czech Academy of Sciences, Institute of Biophysics, Kralovopolska 135, CZ-61265 Brno, Czech Republic
E-mail: brabec@ibp.cz
[b] Prof. J. Ruiz
Departamento de Química Inorgánica,
Universidad de Murcia, and Biomedical Research Institute of Murcia (IMIB-Arrixaca), E-30071 Murcia (Spain)
[c] Prof. Vicente Marchán
Departament de Química Inorgànica i Orgànica,
Secció de Química Orgànica, IBUB, Universitat de Barcelona
Martí i Franqués 1–11, E-08028 Barcelona (Spain)
Supporting information for this article is available on the WWW under https://doi.org/…..

Results and Discussion

Cell sorting and preparation of prostate CSC sub-populations

As indicated in the introductory part, the Ir^{III}–COUPY conjugate **3** was investigated in this study with an intention to identify a new lead compound capable of inhibiting not only proliferation of the prostate differentiated tumor cells but also reducing the tumorigenic capability of prostate CSCs. Therefore, we first focused on identifying and isolating a representative model of prostate CSCs using CSC-specific cell surface markers.[7] An important issue in this research was the identification of representative prostate CSC markers.[8]

Cells from prostate tumors with cancer stem cell characteristics can be identified as sub-populations positive for cell surface markers CD44 and CD133,[9] or CD151 and CD166.[8] Therefore, based on previous studies, we performed multiple tests to find out a phenotypically sorted sub-population of a human prostate cancer cell line DU145 considered to be one of the standard prostate cancer cell lines used in therapeutic research.[10] Isolation of specific sub-populations was carried out by MACS affinity columns, and the sorting purity was further checked by flow cytometry (Figure S1). Moreover, due to their unlimited self-renewal ability, CSCs tend to form tumorspheres in non-adherent, serum-free cell cultures.[11] Thus, the ability of sorted subpopulations to form tumorspheres was assessed by counting formed tumorspheres with a diameter higher than 40 µm (excluding cell clumps; Figure 2).

The flow cytometry data indicated that the highest sorting purity and phenotype distribution was achieved after the affinity sorting of DU145 cells for the CD151 cell surface marker (Figure S1C). CD151 is a member of the transmembrane tetraspanin superfamily, which is essential in regulating cell development, activation, growth, and motility.[8] The other sorted subpopulations (CD44, CD133, CD166) displayed only low distribution between positive and negative phenotypes with a low separation of positive from the negative population (Figures S1A,B,D). The $DU145^{CD151+}$ cell surface marker's overall sorting yield was approximately 1% of the total (unsorted) population.

Since the CSC phenotype can also be confirmed by the ability of CSCs to form tumorspheres,[11] we next focused on determining whether $DU145^{CD151+}$ cell sub-population can effectively form the tumorspheres. The ability of populations of DU145 cells to form tumorspheres was assessed by counting formed tumorspheres with a diameter higher than 40 µm (excluding cell clumps; Figure 2). The cells were seeded as single cells under ultra-low attachment conditions for 96 h, and the number of formed spheroids was analyzed and related to one-thousand seeded cells (Figure 2). The unsorted control population of DU145 cells formed approximately 27±3 spheroids, whereas CD151-negative (-) phenotypes of DU145 cells only formed 16 spheroids (59% of the control). On the other hand, the $DU145^{CD151+}$ cell sub-population formed 38 spheroids. Thus, the CD151-positive sub-population of DU145 cells was taken in the present study as the representative model of the prostate CSCs.

Antiproliferative properties

The anti-proliferative properties of Ir^{III}–COUPY conjugate (**3**) and of the two parent compounds (**1** and **2**) against tumorspheres formed from CD151-positive and negative subpopulations of prostate DU145 cells, both in the dark and under irradiation conditions (420 nm blue light, 28 J cm^{-2}, 30 min), were assessed using the CellTiter-Glo 3D cell viability assay. The sorted subpopulations of single cells were incubated for 96 h to form tumorspheres, which were characterized by round-shaped morphology. The formed spheroids were treated according to the treatment schedule described in detail in the section Materials and methods and further incubated for 70 h in the drug-free medium. The drug dose-response curves were analyzed; the IC_{50} values (the concentration of a drug that gives half-maximal response) are summarized in Table 1. The IC_{50} values determined by this assay were also used to determine phototoxicity and selectivity for the tumor cells and CSC-phenotype selectivity (Table 2).

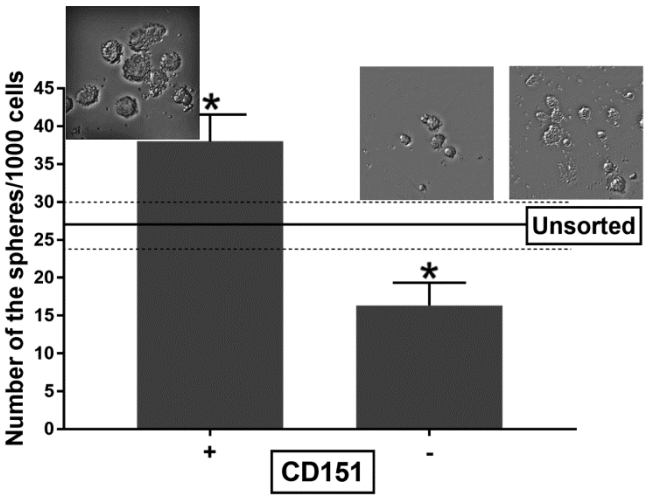

Figure 2. Formation of tumorspheres after the MASC affinity sorting. DU145 cells were sorted for CD151 cell surface markers, and the positive (+) and negative (-) populations were incubated in 3D forming, ultra-low attachment, and non-differentiation conditions for 96 h. The tumorspheres formed were imaged, counted and tumorspheres with the diameter above 40 µm were included in the statistics. The number of the spheres was related to 1000 sorted cells seeded under sphere-forming conditions. Representative bright-field images of sorted subpopulations are at the top of the bars, whereas image for unsorted cells are attached to the level line of control. *Stars indicate a significant difference from unsorted control cells with p≤0.05 calculated using students´ t-test. Four independent experiments were performed, and the ability to form tumorspheres was continuously monitored.

Table 1. Antiproliferative activity of the investigated compounds against prostatic cancer stem cells DU145, CD151-positive or negative phenotypes, and non-malignant cells PNT1a[a]

$IC_{50,72h}$ [µM][b]	DU145 CD151+ Irrad[c]	DU145 CD151+ Dark[d]	DU145 CD151- Irrad[c]	DU145 CD151- Dark[d]	PNT1a unsorted Irrad[c]
1	1.8±0.1	≥100	7±1	≥100	2.8±0.7
2	2.3±0.5	85±4	2.7±0.2	78±6	3.9±0.2
3	5.7±0.2	≥100	5.9±0.6	≥100	13±2

[a] Cell spheroids formed from the sorted or unsorted cells were treated for 2 h (1.5 h of incubation plus 0.5 h of irradiation at the dose of 28 J cm^{-2} of 420 nm blue light) followed by 70 h of incubation in a drug-free medium. Control cells were left in the dark.
[b] The concentration of a compound that gives a half-maximal response determined by using CellTiter-Glo 3D cell viability assay.
[c] The samples were irradiated at the dose of 28 J cm^{-2} of 420 nm blue light for 30 min;
[d] The samples were kept in the dark for 2 h.

According to the IC_{50} values obtained for all investigated compounds (Table 1), the growth of prostate DU145 tumorspheres was inhibited in both CSC-enriched CD151+ and CSC-depleted CD151- after the irradiation with blue light. As spheroids usually show increased resistance to drug treatments compared to the 2D monolayer culture models,[12] the IC_{50} values shown in Table 1 are

encouraging and demonstrate a high antiproliferative activity against the tumorspheres, the IC_{50} values being in a low micromole range. Notably, the dark toxicity was very low and undetectable in the designed concentration range for iridium complex **1** and iridium-coumarin conjugate **3**. By contrast, the coumarin derivative **2** showed moderate toxicity also in the dark. The IC_{50} values in both investigated phenotypes also indicate different responses of the tumorspheres to the tested compounds, supporting the view that the mechanism of action of the investigated compounds in the two phenotypes is different.[13]

In order to determine the most suitable candidate for treating prostate cancer, we next analyzed the results shown in Table 1 in more detail by calculating photoselective and therapeutic indexes. As shown in Table 2, the conjugation of iridium complex **1** to COUPY (compound **2**) forming compound **3** resulted in a compromised photoselectivity. However, it is worth noting that the therapeutic efficacy of the investigated drugs could be also negatively affected by their destructive effects on surrounding non-malignant tissues, which might also be exposed to the irradiation. This is why the highest selectivity towards cancer tissue is usually achieved by the targeted photoactivation. Therefore, we also examined the selectivity against non-malignant tissue and calculated the therapeutic index (TI) (Table 2). The data indicate that the highest therapeutic index was observed for the Ir^{III}–COUPY conjugate (**3**), demonstrating beneficial selectivity of this compound for cancer tissue over non-malignant tissue.

Given that it is desirable to identify anticancer drug candidates that would kill with substantial efficiency both differentiated prostate cancer cells and prostate CSCs, we calculated the CSC-selectivity index (Table 2). The highest CSC-selectivity index was obtained for iridium complex **1**, suggesting a relatively high sensitivity of prostatic DU145 CSCs to this compound. Contrastingly, **2** and **3** were considerably less active against CSC-phenotype, **3** being even equally active in both cancer and CSC-like cells. This activity of **3** has important implications for developing chemotherapeutic agents suitable for the treatment of prostate cancer cells also due to the heterogeneity of prostate gland cancer tissue. Therefore, due to the considerable activity of the investigated compounds in the CD151-positive phenotype of prostate cancer DU145 cells, we sought to gain more insight into their mechanism of action, mainly in the CD151-positive phenotype.

Table 2. Phototoxic, therapeutic, and CSC selectivity of compounds **1** - **3** in prostatic cancer stem cells DU145, CD151-positive or negative phenotypes

	PI[a]		TI[b]		CSC SI[c]
	CD151+	CD151-	CD151+	CD151-	CD151
1	≥55.6	≥14.5	1.6	0.4	3.8
2	36.7	28.7	1.7	1.4	1.2
3	≥17.5	≥16.9	2.2	2.2	1.0

[a] Photoselective index (PI) calculated as $IC_{50,72h}$ obtained for samples incubated in the dark / $IC_{50,72h}$ for cells irradiated with blue light.
[b] Therapeutic index (TI) calculated as $IC_{50,72h}$ for irradiated non-malignant cell line PNT1a / $IC_{50,72h}$ for irradiated malignant cell line DU145, CD-positive (+) or CD-negative (-) phenotype.
[c] CSC selectivity index (CSC SI) calculated as $IC_{50,72h}$ for CD-negative (-) phenotype / $IC_{50,72h}$ for CD-positive (+) phenotype.

Cellular distribution and penetration to tumor mass of prostatic CSCs

The ability to penetrate through tumor mass is one of the determinants affecting the efficiency of anticancer drugs. Tumor spheroids consist of proliferative cells in the periphery, quiescent cells in the intermediate zone, and a necrotic core.[14] Tumor spheroids mimic nonvascularized microtumors, exhibiting similar characteristics with patient metastases.[15] The penetration of the drugs also to the inner shells of tumorspheres may affect the viability and compactness of the spheroids. Disruption and cytotoxic action inside the tumorspheres may enhance the overall anticancer effect of the drugs. The tumorspheres from $DU145^{CD151+}$ (diameter: 90-110 µm) were treated with the investigated compounds and visualized by confocal microscopy in defined z-stack steps. The intensity of the fluorescence signal was expressed in 3D graphs (Figure 3), demonstrating the penetration of compounds inside the tumor mass. Confocal microscopy of $DU145^{CD151+}$ spheroids (Figure 3) revealed fast uptake upon 2 h incubation time. Interestingly, we observed very different trafficking of **1-3** by tumorspheres. Compound **1** penetrated mainly to the shell of the spheres in a depth corresponding to 10-20 µm (which corresponds to the cell layer of one-two cells). In contrast, COUPY derivative **2** penetrated mainly to the intermediate zone of the spheres. The necrotic core was clear from the fluorescence signal yielded by **2** demonstrating the inability of **2** to target necrotic cells inside the spheroids.

On the other hand, the fluorescence signal from Ir-COUPY conjugate **3** was homogenously distributed in the different z-stacks, including over whole deep-seated sections. This observation suggests that **3** can target all proliferative, quiescent, and necrotic cells in the spheroids formed from $DU145^{CD151+}$ CSCs. As we demonstrated previously, the Ir-coumarin conjugate **3** belongs to the class of type I Ir^{III} photosensitizers[16] and thus does not suffer from the typical drawbacks of type II photosensitizers. The type I photosensitizers are less oxygen-sensitive, and therefore their cytostatic activity is also preserved in the hypoxic core of tumor mass. The lower O_2 consumption rate of type I photosensitizers predetermine them to be promising chemotherapeutic agents for low-vascularized hypoxic tumors.[17] Considering the aforementioned, we also determined sub-cellular localization of the investigated compounds immediately after irradiation (Figure S2) and after subsequent 22 h of incubation in the monolayer of $DU145^{CD151+}$ CSCs (Figure S3). We found quite similar localization of **1** and **3** in the cytoplasm of the cells under both irradiation conditions and in the dark immediately after the irradiation and 22 h post-irradiation. Taken together, the results demonstrating the penetration of the investigated compounds inside the tumor mass (Figure 3) indicate that mainly compound **3** can target all sections of the cells in the spheroids formed from $DU145^{CD151+}$ CSCs. This result suggests that among the three investigated compounds, conjugate **3** has the best capability of penetrating through tumor mass of prostate $DU145^{CD151+}$ CSCs.

Apoptotic cell death in prostatic CSCs treated with photoactivated 1-3

Since apoptosis is one of the basic mechanisms of cell death, we next decided to analyze levels of apoptosis in $DU145^{CD151+}$ cells cultured as 3D spheroids (diameter: 90-110 µm) treated with **1-3** at their concentrations in the range of 1 – 10 µM using the RealTime-Glo annexin V apoptosis assay. This assay measures the real-time exposure of phosphatidylserine on the outer leaflet of cell membranes during the apoptotic process. Annexin V luciferase fusion proteins supplied in the assay reagent bind to phosphatidylserine during apoptosis and are detected with a simple luminescence signal. Thus, this assay can follow the dynamics of apoptosis and thus track the fate of the CSC spheroids after treatment with the investigated compounds. In our experiments, the signal was recorded every 1 h over the period of 18 h (shown in

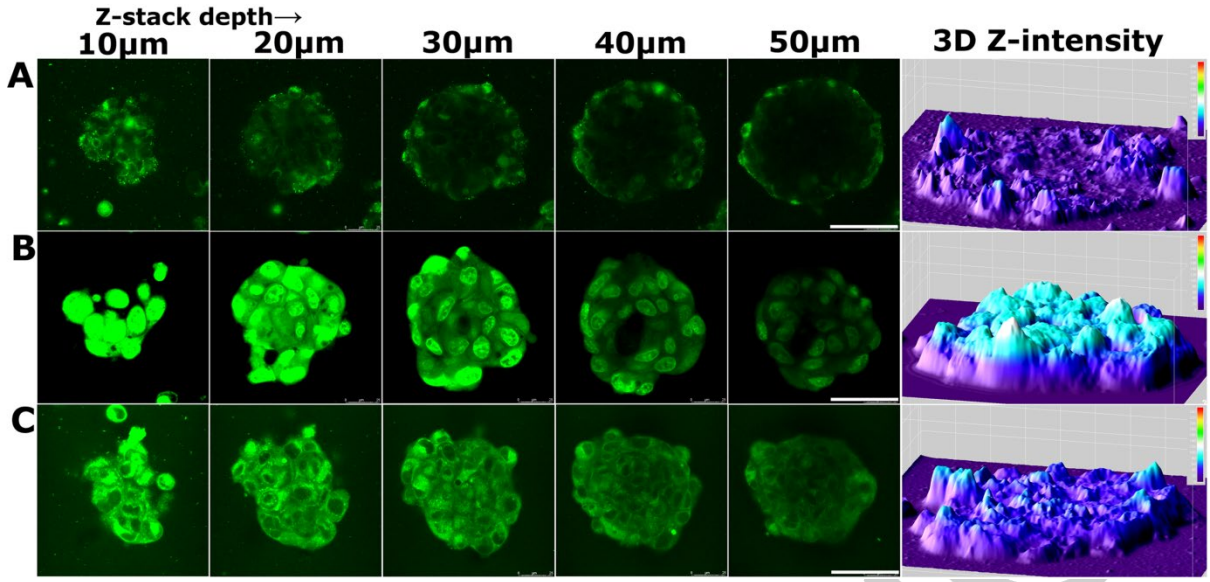

Figure 3. Penetration of compounds **1** - **3** to 3D spheroids generated from DU145^{CD151+} cells. Cell spheroids (diameter: 90-110 µm) were treated with 5 µM of A) **1**, B) **2,** and C) **3**, incubated for 1.5 h in the dark followed by 0.5 h of irradiation with the blue light. Confocal microphotographs were acquired in defined z-stack steps (10-50 µm). Scale bar represents 50 µm. 3D graphs on the right side of the Figure represent fluorescence intensity distribution through the spheroid mass.

Figure 4 for the treatment with 2 µM **1** – **3**). The apoptotic process in the tumorspheres from DU145^{CD151+} cells (diameter: 90-110 µm)treated with **1** – **3** was initiated soon after the irradiation. The most effective compound inducing apoptosis was **1**, and the trend was **1**>**2**>**3**. The same trend, which correlates with their antiproliferative activity in prostate DU145^{CD151+} tumorspheres (Table 1), was observed if the spheroids were also treated with **1** – **3** at the concentration of 1, 5, and 10 µM.

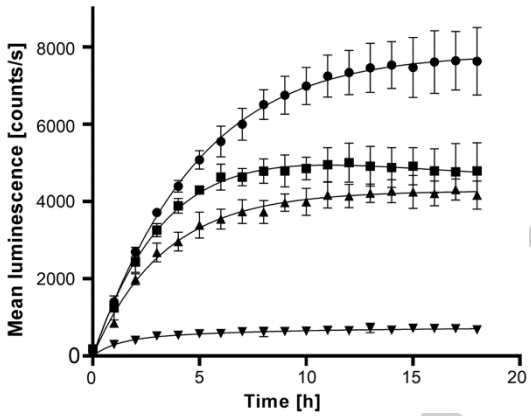

Figure 4. Real-time apoptosis assay. Tumorspheres from DU145^{CD151+} cells (diameter: 90-110 µm) were treated for 2 h with **1** – **3** at the concentration of 2 µM (1.5 h of incubation in the dark plus 0.5 h of irradiation at the dose of 28 J cm^{-2} of blue light). Subsequently, the samples were assayed by RealTime-Glo^{TM} annexin V apoptosis assay every 1 h over the period of 18 h. ▼, control; ●, **1**; ■, **2**; ▲, **3**. Results are expressed as the mean luminescence. Time 0 h represents the initial value after the irradiation of samples treated with the tested compounds.

Calcium signaling flux

The results of the analysis of levels of apoptosis in prostate cancer DU145^{CD151+} cells cultured as 3D spheroids treated with **1**-**3** (Figure 4) revealed the importance of apoptosis in the mechanism of action of the investigated compounds in prostate CSCs. The mechanism of apoptosis is complex, involves many pathways, and those involving calcium ion (Ca^{2+}) dependent mechanisms required for activation of an apoptotic cascade have been intensively investigated in recent years. Notably, perturbation of Ca^{2+} homeostasis induced to undergo apoptosis by a variety of agents, including chemotherapeutics, commonly occurs also in prostate cancer cells and CSCs.[18] The intracellular cytosolic concentration of calcium ions is physiologically maintained at very low concentrations. However, specific conditions (cell death pathways, intracellular signaling, etc.) can initiate rapid elevation of intracellular calcium by release from calcium stores in organelles, mainly the endoplasmic reticulum.[19] These changes can be analyzed by a calcium signaling assay.

Therefore, we next decided to test calcium signaling flux in prostate cancer DU145^{CD151+} CSC model and its contribution to the cell death induced after the treatment of the tumorspheres from DU145^{CD151+} cells with compounds **1** – **3** (Figure 5). Ionophore ionomycin was used as a positive control for its known impact on Ca^{2+} flux across the plasma membrane and transport of Ca^{2+} out of the intracellular stores into the cytosol.[20]

The tumorspheres from DU145^{CD151+} (diameter: 90-110 µm) were treated with the investigated compounds at equitoxic (2x$OC_{50,72h}$, Table 1) (Figure 5A) or various equimolar concentrations (Figure 5B) for 1.5 h under dark conditions followed by 30 min of blue-light irradiation. Then, the cells were incubated in a drug-free medium loaded with Fluo-4 AM Ca^{2+} detection probe, and the fluorescence signal was acquired every 15 min over the time period of 2 h. The data depicted for samples exposed to equitoxic concentrations (2x$IC_{50,\ 72h}$) (Figure 5A) indicate an immediate Ca^{2+} flux after the irradiation as a response to **1**, **2**, **3**, and ionomycin treatment. After 15 min incubation in the cell-free medium, the levels of Ca^{2+} were comparable for all of the tested compounds. The amount of Ca^{2+} still increased over the investigated period of time with an approximate increase of 3-9% every 15 min. The stimulation of Ca^{2+} flux was also dependent on the concentration of the compounds, as indicated in Figure 5B. The cell response recorded 15 min after the irradiation in terms of Ca^{2+} release was saturated after the treatment with 5 µM (2x$IC_{50,\ 72h}$) of **1** and **2**, whereas **3** saturates the response of DU145^{CD151+} CSC at the concentration of 20 µM (4x$IC_{50,\ 72h}$). The positive control ionomycin showed a continuous increase of Ca^{2+} flux in the studied concentration range. Overall, the data indicate that the Ca^{2+} signaling flux goes hand in hand with the apoptotic process after the treatment with the

investigated compounds. The identification of the initial intracellular source of Ca^{2+} signaling flux, which is a very complex process, was behind the scope of our study and will be carried out in our future study.

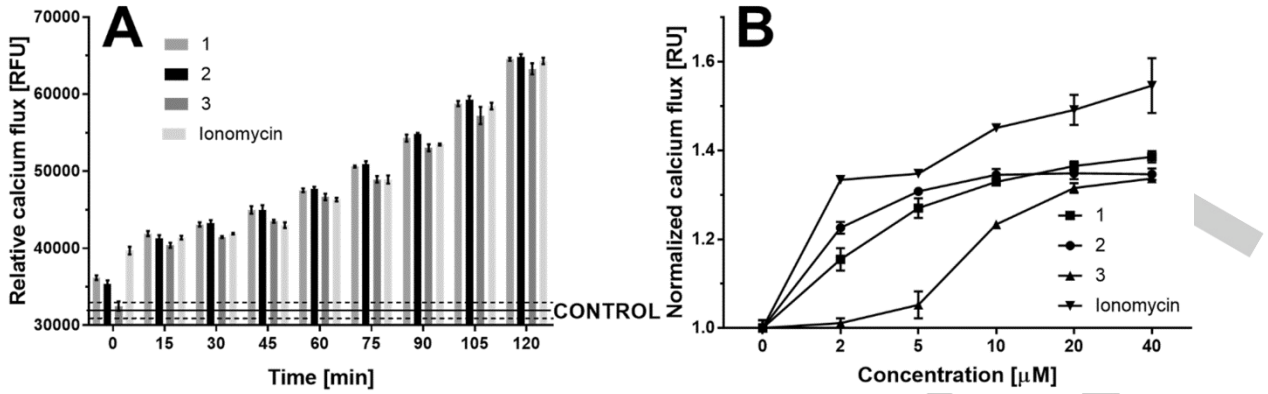

Figure 5. Calcium signaling flux. A. Kinetic measurement of calcium flux in the tumorspheres from DU145^{CD151+} cells treated with equitoxic concentrations (2x$IC_{50,72h}$) of the investigated compounds. The line marked as CONTROL indicates the level of Ca^{2+} in the untreated control samples. B. Concentration dependence of the calcium flux analyzed 15 min after the irradiation of DU145^{CD151+} tumorspheres.

Stimulation of autophagy in prostatic CSCs

We have demonstrated the role of Ca^{2+} in apoptosis induced in the tumorspheres from the prostatic DU145^{CD151+} cells (Figure 5) by all the investigated compounds (**1**-**3**). However, cytosolic Ca^{2+} upload, which represents one of the stressful conditions, has been shown to activate autophagy, maintained at a low basal level in most cells. Autophagy is a self-digestion process of the cells developed for degradation and recycling of proteins, damaged organelles, and lipids, thereby acting as a control mechanism of cellular homeostasis. Notably, it is generally accepted that autophagy represents a promising approach to counteract CSCs aggressiveness[21] and that this role of autophagy is connected with Ca^{2+}-dependent signaling pathways.[22] However, contradictory roles of Ca^{2+} in the process of autophagy have been proposed.[21, 23] Next, we sought to gain more insight into the relationship between Ca^{2+} signaling, autophagy, and chemotherapy by the investigated compounds targeted against prostatic CSCs. Thus, the aim of the following experiments was to examine whether autophagy has an impact on the mechanism of action of the compounds **1**-**3**. To do so, we treated tumorspheres formed from DU145^{CD151+} prostatic CSCs with equitoxic concentrations of the tested compounds corresponding to 2 or 5x$IC_{50,72h}$ for 24 h. The data were compared with the effects of the established autophagy stimulators rapamycin and chloroquine. Samples were stained with a Cyto-ID autophagy detection probe and analyzed by flow cytometry (Figure 6). Compounds **1**-**3** did not initiate statistically significant autophagy in DU145^{CD151+} prostatic CSCs in the dark. After the irradiation, autophagy was activated in DU145^{CD151+} prostatic CSCs treated with **1** or **3**, whereas the treatment with the COUPY coumarin derivative **2** remained ineffective. Moreover, Ir-COUPY conjugate **3** under irradiation conditions stimulated autophagy even more effectively than the combination of established autophagy stimulators rapamycin and chloroquine used as recommended by the manufacturer. Very interestingly, whereas the three investigated compounds **1**-**3** stimulated both Ca^{2+} flux and concomitantly also induced apoptosis in DU145^{CD151+} prostatic CSCs (Figures 4 and 5), the autophagy was only stimulated by the Ir complex (**1**) and the conjugate (**3**), **3** being markedly more effective (Figure 6). This observation is consistent with the view and supports the hypothesis that the autophagy-initiation process induced, in particular by Ir-coumarin conjugate **3**, is mainly connected with the presence of iridium moiety. Taken together, whereas the mechanism of cell death in DU145^{CD151+} prostatic CSCs induced by coumarin derivative **2** involves mainly induction of apoptosis, that induced by **1** or **3** is mediated by both apoptotic and autophagic cell death pathways. The important implication of this finding might be that development of resistance pathways against both cell death modes in prostatic both differentiated and stem cancer cells might be less likely when using Ir-COUPY conjugates as chemotherapeutic agents**.**

Generation of ROS in prostatic CSCs

Oxidative stress is reported as a common mediator of cell death, including apoptosis.[24] An imbalance between the generation of ROS and intracellular antioxidant defense systems causes cell damage directly or through altering signaling pathways.[25] Cancer cells exhibit higher intracellular levels of ROS, which are counteracted by sophisticated antioxidant mechanisms. Therefore, the physiological saturation of antioxidant machinery in cancer cells makes them very sensitive to ROS-based therapies that stimulate the level of oxidative stress over the tolerable dose. A limited number of studies have been only dedicated to the treatment of CSCs with ROS-based therapies. However, there is emerging evidence that ROS is essential for regulating the self-renewal and differentiation ability of CSCs.[26] It has been shown in our previous study that compounds **1** - **3** are very effective in stimulation of intracellular ROS,[6] however, their efficiency to stimulate oxidative stress in prostatic CSCs has not been tested. Thus, we decided to quantify ROS's level in tumorspheres formed from prostatic DU145^{CD151+} and DU145^{CD151-} cells treated with the investigated compounds. The tumorspheres were treated with the equitoxic concentrations of **1** - **3** corresponding to 5x$IC_{50,72h}$ and incubated for 1.5 h under the dark conditions followed by 0.5 h of irradiation with 420 nm blue light (28 J cm^{-2}).

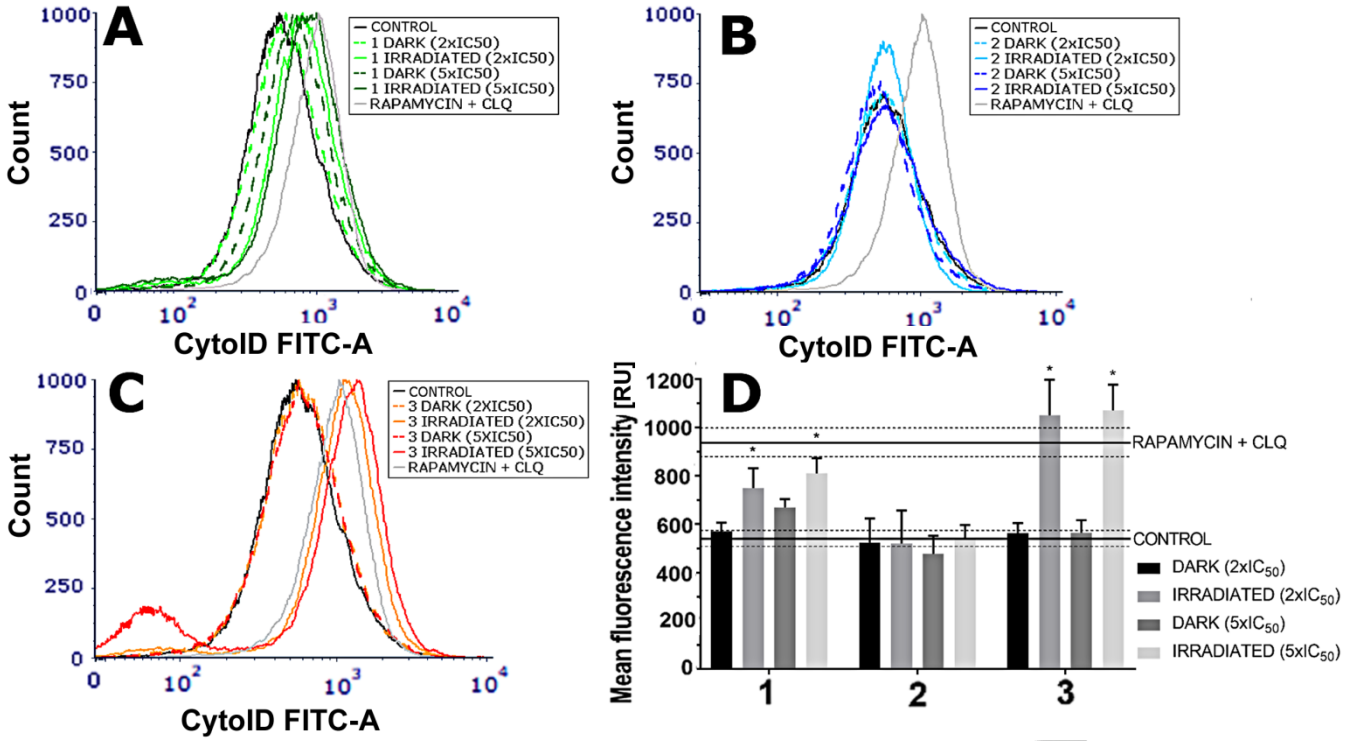

Figure 6. Flow cytometry-based profiling of autophagy in tumorspheres formed from prostatic DU145^{CD151+} cells. The tumorspheres were untreated (control), treated with equitoxic concentrations of **1**-**3** corresponding to their 2x or 5xIC$_{50,72h}$ or combination of 500 nM rapamycin and 100 μM chloroquine. The samples treated with **1**-**3** were incubated for 1.5 h in the dark, followed by 0.5 h of irradiation with blue light. Subsequently, the samples were incubated for an additional 22 h in a drug-free medium. The samples treated with positive autophagy stimulators, rapamycin (500 nM) and chloroquine (100 μM), were incubated for 18 h. After staining with the CYTO-ID autophagy detection probe, cells were washed and analyzed by flow cytometry. Results are presented as histogram overlays for the effects of **1** (A), **2** (B), and **3** (C). The overall mean fluorescence was quantified and depicted on the panel D.

Relatively high concentrations of **1** - **3** (5xIC$_{50,72h}$) and short exposure time (only 1.5 h under the dark conditions followed by 0.5 h of irradiation with 420 nm blue light (28 J cm^{-2}) were chosen in these experiments. We verified that under these conditions, the cells displayed not less than 95% viability (trypan blue test) at the moment of harvesting. The ability of **1** - **3** to increase the level of intracellular ROS to lethal dose was evaluated using CellRox® reagent and the samples were analyzed by flow cytometry (Figures 7 and S4). We identified Ir-COUPY conjugate **3** as the most efficient stimulator of the oxidative stress in both subpopulations of DU145 cells, the trend being **3**>**2**>**1**. Interestingly, we also found no marked difference in the level of ROS in CD151-positive sub-population of DU145 cells compared to the CD151-negative sub-population. Our findings also demonstrated that when **1**-**3** were applied at equitoxic concentrations, the lowest stimulation of oxidative stress in DU145 cells was shown for **1** despite the fact that **1** exhibited the highest antiproliferative activity (lowest IC$_{50}$, Table 1). On the other hand, the highest efficiency of **3** to increase the level of intracellular ROS (Figure 7) correlates well with its highest efficiency to induce autophagy in DU145^{CD151+} prostatic CSCs (Figure 6). Thus, one can envision scenarios in which autophagy and stimulation of oxidative stress play an important role in the mechanism of action of Ir-coumarin conjugate **3**.

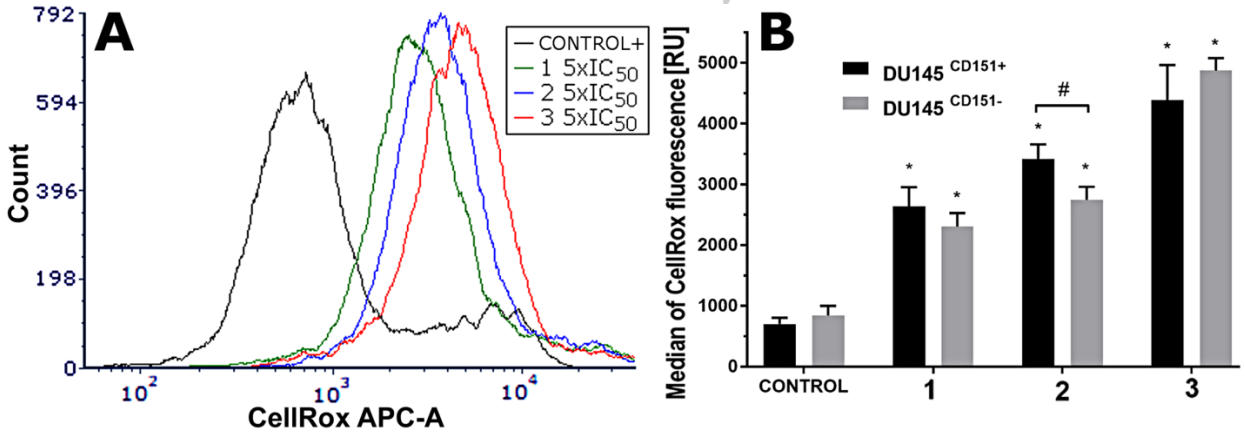

Figure 7. Generation of ROS in DU145^{CD151+} or DU145^{CD151-} cells determined by flow cytometry. Tumor spheroids were treated with equitoxic concentrations of the investigated compounds corresponding to 5xIC$_{50,72h}$ for 2 h (1.5 h in the dark followed irradiation with 420 nm blue light (28 J cm^{-2}) for 0.5 h, and the ROS were quantified by using CellRox® reagent. A. Representative flow cytometry histograms for quantification of ROS in DU145^{CD151+}. B. Comparative bar chart depicting the levels of ROS generated in DU145^{CD151+} or DU145^{CD151-}. Experiments were repeated in duplicate and (*) denote a statistically significant difference from the untreated control or (#) the significant difference in the effects in the respective CD151-positive or CD151-negative subpopulation. Statistical analysis was calculated by using the non-parametric Kruskal-Wallis test with p≤0.05.

Conclusions

We recently demonstrated [6] that a conjugate between a photoactivatable cyclometalated Ir^{III} complex and a far-red-emitting coumarin, Ir^{III}–COUPY (**3**), is a very promising photosensitizer (PS) suitable for photodynamic therapy of cancer, including for the treatment of hypoxic tumors. Therefore, the primary goal of this work was to deepen knowledge on the mechanism of its photoactivated antitumor action and use this knowledge to propose a new class of photoactivatable compounds as drug candidates for curing very hardly treatable human tumors, such as androgen resistant prostatic tumors of metastatic origin. The impetus for the studies described in this report was that photocytotoxicity of **3** is connected with its ability to generate a specific type I ROS in living cells, superoxide anion radical, upon visible-light irradiation.[6] This property predisposed conjugate **3** to become an efficient PS agent capable of killing not only the bulk of cancer cells but also hardly treatable CSCs responsible for cancer recurrence and the metastatic progression of cancer.[5]

The activity of Ir^{III}–COUPY conjugate **3** as well as that of its parent compounds (Ir^{III} complex **1** and COUPY **2**) for comparative purposes was tested in CSC-enriched and CSC depleted DU145 taken in this study as the model of hormone-refractory and aggressive prostate cancer cells, which are resistant to conventional antineoplastic drugs. The investigated compounds photoactivated by blue light exhibited a promising antiproliferative activity in both CSC-enriched and CSC-depleted DU145 cells in a low micromolar range, **3** being slightly less active (Table 1). Thus, the conjugation of **1** and **2** forming **3** does not lead to the synergistic overall antiproliferative effects of the parental compounds. It results in the ability of **3** to penetrate all sections of the cells in tumors and beneficial selectivity of **3** for cancer tissue over non-malignant tissue. All the compounds demonstrated a high photoselectivity (Table 2). Importantly, in particular, photoactivated conjugate **3** showed the highest selectivity for prostate tumor cells DU145 compared with noncancerous cells (Table 2), which is an important feature since its application to prostate cancer patients would diminish the damage of healthy cells in close proximity of the tumor. The fact that conjugate **3** exhibited equal activity in CSC-depleted and CSC-enriched DU145 prostate cancer cells (Table 2) indicates that it may be equally effective in killing both cells in the bulk of tumor and CSCs simultaneously. This may be highly advantageous for the chemotherapy of prostate cancer since this property of **3** may minimize the use of more specialized chemotherapeutics in combination to cure prostate cancer and can be switched on by visible light irradiation.

On the other hand, all investigated compounds induced apoptotic cell death in prostate cancer DU145 cells (Figure 4) associated with calcium signaling flux in these cells (Figure 5). Very interestingly, Ir-COUPY conjugate **3** and, to a considerably smaller extent also **1**, in contrast to **2**, also induced autophagy in prostate cancer DU145 cells (Figure 6). This observation correlates with the highest efficiency of conjugate **3** to induce in DU145 prostate cells oxidative stress (Figure 7). Autophagy has been shown to potentiate the cytotoxicity of chemotherapeutic drugs but has also been linked to drug resistance.[27] Work is in progress to determine the role of autophagy in the mechanism of antitumor effects of **3**.

In summary, it is reasonable to conclude that Ir-COUPY conjugate **3** combines biologically interesting properties of both parent compounds **1** and **2**. Nevertheless, the results of our study suggest that the mechanism of cytotoxicity *in vitro* of conjugate **3** is different from that of **1** and **2**. The cyclometalated Ir^{III} complex moiety **1** seems to be responsible for autophagic response and photoselectivity of **3**, whereas coumarin derivate COUPY **2** for the enhanced generation of ROS. The combination of both parent compounds also lead to a considerable increase of the capability of the resulting conjugate **3** to penetrate the inner layers of tumorspheres (Figure 3), which might markedly increase its therapeutic effect. This study also shows that Ir^{III}-COUPY conjugate **3** has a great potential for photodynamic therapy of hardly treatable, hormone-refractory, and aggressive prostate cancer. This is because the photoactivated conjugate affects very efficiently and simultaneously both the cells in the bulk of the tumor and CSCs. Within the context of studies with photoactivatable antitumor metallodrugs, we have shown for the first time that the photoactivatable metal-based compound is an efficient agent capable of killing even hardly treatable CSCs. In addition, the very low toxicity of **3** in the prostate DU145 cells in the dark and its pronounced selectivity for tumor cells compared with noncancerous cells could result in low side effects and reduced damage of healthy cells during the photoactivated therapy by Ir^{III}-COUPY conjugate **3**.

Experimental Section

Cell lines and cultivation. DU145 cells were purchased from ATCC (American Type Culture Collection, USA). PNT1a were from ECACC (European Collection of Authenticated Cell Cultures, England). Spheroids generated from cell cultures and sorted subpopulations were cultured in 3D forming, non-differentiation, ultra-low attachment conditions in the non-differentiation DMEM-F12 Ham medium supplemented with 2% B27 (Thermo Fisher Scientific Inc., MA, USA), epidermal growth factor (EGF; Sigma Aldrich, Germany, 20 ng mL^{-1}), fibroblast growth factor (FGF2; Sigma Aldrich, Germany,10 ng mL^{-1}) and bovine serum albumin (BSA) (Sigma Aldrich, Germany, 0.15%). Ultra-low attachment cell culture plastics were from Corning (NY, USA).

Cell sorting and preparation of prostate CSC sub-populations. Sub-populations from DU145 cells were isolated using the MACS affinity sorting procedure. Cells were sorted for surface markers CD44, CD133, CD151, and CD166, all from Miltenyi Biotec, Gladbach, Germany). Sub-populations with positive and negative phenotypes were used for further experiments. Phenotypical distribution of subpopulations was analyzed using flow cytometry on BD FACS Verse (BD Biosciences, USA).

Formation of tumorspheres. Sorted subpopulations were analyzed for their tumorsphere formation ability. For this purpose, cells were seeded on the 96w ULA plates at the density of 1000 cells/well, and the number of formed spheroids was analyzed 96 h post-seeding on multimode reader SPARK (Tecan, Austria).

Monitoring the antiproliferative effects of the investigated compounds. Sorted sub-populations were seeded on 96w ULA plates and incubated for 96 h to form the spheroids under the non-differentiated conditions. Then, the spheroids were centrifuged (200 g, 2 min), and the culture non-differentiation media was replaced by Dulbecco's phosphate-buffered saline (DPBS) supplemented with increasing concentrations of the investigated compounds. Cells were incubated for 1.5 h in the dark and then irradiated with 420 nm blue light (28 J cm^{-2}) for 30 min; control samples were stored in the dark. The cells were subsequently centrifuged (200 g, 2 min), and the DPBS solutions were replaced by the non-differentiation medium. Cells were incubated for a further 70 h, and at the end of the incubation period, wells were loaded with an equal amount (100 µL) of CellTiter-Glo® 3D (Promega, WI, USA). Luminescence signal was detected on multimode reader SPARK (Tecan, Manedorf, Swi). The IC_{50} values were calculated from the survival curves. Experiments were repeated in triplicate.

Cellular distribution and penetration of the investigated compounds to tumor mass of prostatic CSCs. $DU145^{CD151+}$ cells were seeded on 6w plates at the density of $1.5x10^5$ cells/well and cultured for 96 h to form spheroids. The spheroids were subsequently treated with the investigated compounds (5 µM) for 1.5 h, followed by irradiation with 420 nm blue light for 0.5 h. The spheroids were centrifuged/washed (200 g, 2 min/PBS). Samples were fixed with 4% formaldehyde and replaced on 35 mm confocal dishes (Mattek, USA), with subsequent immobilization with Vectashield hard set (Thermo Fisher Scientific Inc., MA, USA). Samples were visualized with confocal microscope Leica TCS SP8 SMD (Leica microsystems GmbH, Wetzlar, Germany). The defined 10 µm z-stack

steps were used for visualization of tumor-mass drug penetration. Images and 3D fluorescence intensity graphs were processed in ImageJ studio (NIH, Wisconsin, USA).

Time-dependent apoptotic response to the treatment of prostatic CSCs. DU145^{CD151+} cells were seeded on 96w ULA plates at the density of 1x10^3 cells/well and cultured for 96 h to form spheroids. The spheroids were treated in DPBS with increasing concentrations of the tested compounds for 1.5 h, followed by irradiation with 420 nm blue light (28 J cm^{-2}) for 0.5 h. Real-time apoptosis was analyzed using the RealTime-Glo™ Annexin V apoptosis assay (Promega, USA). Luminescence signal coming from NanoBit® luciferase was monitored for 25 h post-treatment by using multimode reader SPARK (Tecan, Austria).

Calcium signaling flux. DU145^{CD151+} cells were seeded on 96w ULA plates at the density of 1x10^3 cells/well and cultured for 96 h to form spheroids. The spheroids were treated in DPBS with increasing concentrations of the investigated compounds for 1.5 h, followed by irradiation with 420 nm blue light (28 J cm^{-2}) for 0.5 h. Ionophore ionomycin was used as the positive control. Calcium signaling flux was monitored using Fluo-4 AM (Thermo Fisher Scientific Inc., MA, USA) in a drug-free medium immediately after the irradiation for a further 2 h. The fluorescence signal (Exc. 455 nm/Em. 510 nm) was monitored using multimode reader SPARK (Tecan, Austria).

Stimulation of autophagy in prostatic CSCs. Autophagy was analyzed in DU145^{CD151+} cells treated with equitoxic concentrations of the investigated compounds corresponding to 2x or 5x$IC_{50,72h}$. Samples were incubated for 1.5 h in the dark, followed by irradiation with blue light for 0.5 h. Samples were incubated for a further 22 h in a drug-free medium. The samples treated with positive autophagy stimulators, rapamycin (500 nM) and chloroquine (100 μM), were incubated for 18 h. Cyto-ID2 probe (Enzo Life Sciences, USA) was used to monitor autophagy, and the samples were analyzed by flow cytometry BD FACS Verse (BD Biosciences, USA). Data were managed in FCS Express software (DeNovo Software, CA).

Generation of ROS in prostatic CSCs. DU145^{CD151+} cells were seeded on 6w ULA plates at the density of 1x10^5 cells/well. Cells were incubated under the non-differentiating conditions for 96 h to form 3D spheroids. The spheroids were treated with equitoxic concentrations of the investigated compounds corresponding to 5x $IC_{50,72h}$ and incubated for 1.5 h in the dark, followed by irradiation with 420 nm blue light (28 J cm^{-2}) for 0.5 h. The spheroids were subsequently harvested, centrifuged (200 g, 2 min), washed with PBS, and then incubated with CellRox ROS detection reagent (Thermo Fisher Scientific Inc., MA, USA). Samples were analyzed by flow cytometry BD FACS Verse (BD Biosciences, USA). Data were managed in FCS Express software (DeNovo Software, CA).

Statistical analysis. Data were analyzed in Statistica software (TIBCO Software Inc., USA). If not stated otherwise, the zero hypothesis was defined with a p≤0.05. Data with standard distribution were analyzed using student´s T-test, or one way ANOVA, data with non-standard distribution were subjected to the Kruskal-Wallis test.

Supporting Information

Sorting of DU145 cells (Figure S1), cellular localization of tested compounds in DU145^{CD151+} single cells (Figures S2 and S3), generation of ROS in DU145^{CD151-} cells (Figure S4).

Acknowledgements

This work was supported by the Czech Science Foundation [grant number 21-27514S] and the Spanish Ministerio de Ciencia e Innovación (MCI/AEI) (grant CTQ2017-84779-R).

Conflict of interest

The authors declare no conflict of interest.

Keywords: iridium · coumarin photoactivation · prostate cancer · cancer stem cells · apoptosis · antitumor agents · oxidative stress

[1] E. Nevedomskaya, S. J. Baumgart, B. Haendler, *Int. J. Mol. Sci.* **2018**, *19*, 1359.
[2] U. Swami, T. R. McFarland, R. Nussenzveig, N. Agarwal, *Trends Cancer* **2020**, *6*, 702-715.
[3] a) C. E. Eyler, J. N. Rich, *J. Clin. Oncol.* **2008**, *26*, 2839-2845; b) H. Liu, L. Lv, K. Yang, *Am. J. Cancer Res.* **2015**, *5*, 880-893.
[4] a) X. Qian, X. Nie, W. Yao, K. Klinghammer, H. Sudhoff, et al., *Seminars Cancer Biol.* **2018**, *53*, 248-257; b) Y. S. Kim, M. J. Kang, Y. M. Cho, *Anticancer Res.* **2013**, *33*, 4469-4474.
[5] H. Zhang, J.-Q. Mi, H. Fang, Z. Wang, C. Wang, et al., *Proc. Natl. A cad. Sci. USA* **2013**, *110*, 5606-5611.
[6] V. Novohradsky, A. Rovira, C. Hally, A. Galindo, G. Vigueras, et al., *Angew. Chem. Int. Ed.* **2019**, *58*, 6311-6315; *Angew. Chem.* **2019**, *131*, 6377-6381.
[7] J.-Y. Zhou, M. Chen, L. Ma, X. Wang, Y.-G. Chen, et al., *Oncotarget* **2016**, *7*, 7657-7666.
[8] V. K. Rajasekhar, L. Studer, W. Gerald, N. D. Socci, H. I. Scher, *Nature Commun.* **2011**, 2, 162.
[9] A. T. Collins, P. A. Berry, C. Hyde, M. J. Stower, N. J. Maitland, *Cancer Res.* **2005**, *65*, 10946-10951.
[10] F. Alimirah, J. Chen, Z. Basrawala, H. Xin, D. Choubey, *FEBS Lett.* **2006**, *580*, 2294-2300.
[11] G. Dontu, W. M. Abdallah, J. M. Foley, K. W. Jackson, M. F. Clarke, et al., *Genes Dev.* **2003**, *17*, 1253-1270.
[12] C. J. Lovitt, T. B. Shelper, V. M. Avery, *Biology* **2014**, *3*, 345-367.
[13] R. Leão, C. Domingos, A. Figueiredo, R. Hamilton, U. Tabori, et al., *Urol. Int.* **2017**, *99*, 125-136.
[14] M. Millard, I. Yakavets, V. Zorin, A. Kulmukhamedova, S. Marchal, et al., *Int. J. Nanomedicine* **2017**, *12*, 7993-8007.
[15] R. M. Sutherland, *Science* **1988**, *240*, 177-184.
[16] V. Novohradsky, G. Vigueras, J. Pracharova, N. Cutillas, C. Janiak, et al., *Inorg. Chem. Front.* **2019**, *6*, 2500-2513.
[17] C. L. Evans, A. O. Abu-Yousif, Y. J. Park, O. J. Klein, J. P. Celli, et al., *Plos ONE* **2011**, *6*, e23434.
[18] a) M. C. Marin, A. Fernandez, R. J. Bick, S. Brisbay, L. M. Buja, et al., *Oncogene* **1996**, *12*, 2259-2266; b) D. O'Reilly and P. Buchanan, *Cell Calcium* **2019**, *81*, 21-28.
[19] D. E. Clapham, *Cell* **2007**, *131*, 1047-1058.
[20] J. P. Kao, G. Li, D. A. Auston, *Methods Cell. Biol.* **2010**, *99*, 113-152.
[21] F. Nazio, M. Bordi, V. Cianfanelli, F. Locatelli, F. Cecconi, *Cell Death Differ.* **2019**, *26*, 690-702.
[22] E. Terrié, V. Coronas, B. Constantin, *Cell Calcium* **2019**, *80*, 141-151.
[23] M. D. Bootman, T. Chehab, G. Bultynck, J. B. Parys, K. Rietdorf, *Cell Calcium* **2018**, *70*, 32-46.
[24] T. Ozben, *J. Pharmaceut. Sci.* **2007**, *96*, 2181-2196.
[25] A. Yilmazer, *Biotechnol. Rep.* **2018**, *17*, 24-30.
[26] a) J. Liu, Z. Wang, *Oxid. Med. Cell. Longev.* **2015**, *2015*, 294303; b) S. Ding, C. Li, N. Cheng, X. Cui, X. Xu, et al., *Oxid. Med. Cell.Longev.* **2015**, *2015*, 750798.
[27] H. Liu, Z. He and H.-U. Simon in *The role of autophagy in cancer and chemotherapy*, (Ed. M. A. Hayat), Academic Press, San Diego, **2016**, pp. 253-265.

Entry for the Table of Contents

FULL PAPER

A cyclometalated Ir^{III} complex conjugated to a far-red-emitting coumarin, Ir^{III}–COUPY, is a very promising photosensitizer suitable for photodynamic therapy of cancer. It efficiently eliminates both prostate bulk, differentiated and prostate, hardly treatable cancer stem cells simultaneously and with a similar efficacy. Thus, photo-induced therapy with Ir^{III}–COUPY conjugates, such as photodynamic therapy, might provide a new approach for prostate cancer treatment.

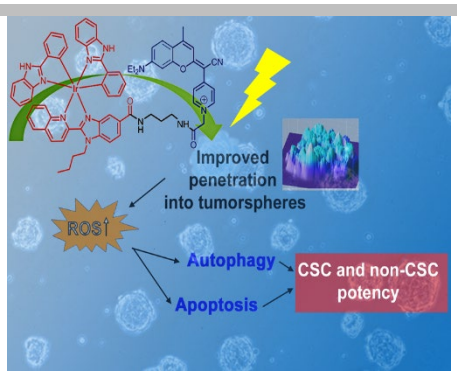

Vojtech Novohradsky, Lenka Markova, Hana Kostrhunova, Jana Kasparkova, Jose Ruiz, Vicente Marchán and Viktor Brabec*

Page No. – Page No.

A Cyclometalated Ir^{III} Complex Conjugated to a Coumarin Derivative Is a Potent Photodynamic Agent against Prostate Differentiated and Tumorigenic Cancer Stem Cells